J Comp Physiol A (1993) 173:445–454

Journal of Comparative Physiology A Sensory, Neural, and Behavioral Physiology

The neural basis of catalepsy in the stick insect

IV. Properties of nonspiking interneurons

R.B. Driesang, A. Büschges

Fachbereich Biologie, Universität Kaiserslautern, D–67663 Kaiserslautern, Germany

Accepted: 18 June 1993

Abstract. The known nonlinearities of the femur-tibia control loop of the stick insect *Carausius morosus* (enabling the system to produce catalepsy) are already present in the nonspiking interneuron E4: (1) The decay of depolarizations in interneuron E4 following slow elongation movements of the femoral chordotonal organ apodeme could be described by a single exponential function, whereas the decay following faster movements had to be characterized by a double exponential function. (2) Each of the two corresponding time constants was independent of stimulus velocity. (3) The relative contribution of each function to the total amount of depolarization changed with stimulus velocity. (4) The characteristics described in (1)–(3) were also found in the slow extensor tibiae motoneuron. (5) Single electrode voltage clamp studies on interneuron E4 indicated that no voltage dependent membrane properties were involved in the generation of the observed time course of decay. Thus, we can trace back a certain behavior (catalepsy) to the properties of an identified, nonspiking interneuron.

Key words: Intrinsic properties – Voltage clamp analysis – Nonspiking interneurons – Joint control – Stick insect

Introduction

Within the last two decades, many investigations have tried to elucidate the neural basis of behavior, i.e. they have tried to trace back parts of its performance to the action of identified neurons in the underlying neural network. This has been particularly successfull in the case of simple behaviors in invertebrates. The crustacean stomatogastric system (e.g. Harris-Warrick et al. 1992), the locust flight system (e.g. Robertson and Pearson 1985; Wolf 1991) and the escape system of the cockroach (e.g. Ritzmann and Pollack 1990) are three impressive examples. Other simple behaviors that have been investigated in great detail are leg reflexes. Leg reflexes are generated by neural control loops governing the leg joints in walking invertebrates (for the crayfish: e.g. El Manira et al. 1991a, b; for the locust: e.g. Burrows 1989, 1992; for the stick insect: e.g. Bässler 1983a, 1993; Büschges 1990). Much is known about the physiology and connectivity of neurons within such control loops. However, little is known about the detailed contribution of identified neurons to the generation of specific behaviors produced by those loops. In most cases this arises from the fact that the behavioral relevance of a particular control loop is not known.

This behavioral relevance is only known for the properties of the joint control loops in the stick insect. E.g. Godden (1974) and Bässler (summary: 1983a) have shown that the control loop governing the femur-tibia joint (FT-joint) in the stick insect generates catalepsy. Catalepsy is a behavioral component of twig mimesis. It means that after a leg was passively forced into a certain position it seems for a casual observer to remain in this position after it is free to move. In reality, it returns to its original position with an extremely low velocity. To perform catalepsy, a joint control loop must be predominantly velocity-sensitive (Bässler and Foth 1982; Bässler 1983a, b). The motoneuronal activity developed during an imposed movement of the FT-joint (resistance reflex) must decline rapidly after a fast bending of the joint, but it must decline very slowly after a slow bending. This nonlinearity produces a high gain for very low stimulus velocities. In other words: For the generation of an effective catalepsy the time course of decline of the feedback response (resistance reflex) must depend on stimulus velocity (for details see Bässler 1983a, 1993). The femur-tibia control loop (FT-control loop) of stick insects fulfills these criteria and is thus adapted to the production of catalepsy (Bässler et al. 1982; Bässler 1983a, b): The faster a passive flexion the greater is the

Abbrevations: FETi, fast extensor tibiae motor neuron; FT-joint, femur-tibia joint; FT-control loop, femur-tibia control loop; SETi, slow extensor tibiae motor neuron; R, regression coefficient

Correspondence to: Robert B. Driesang

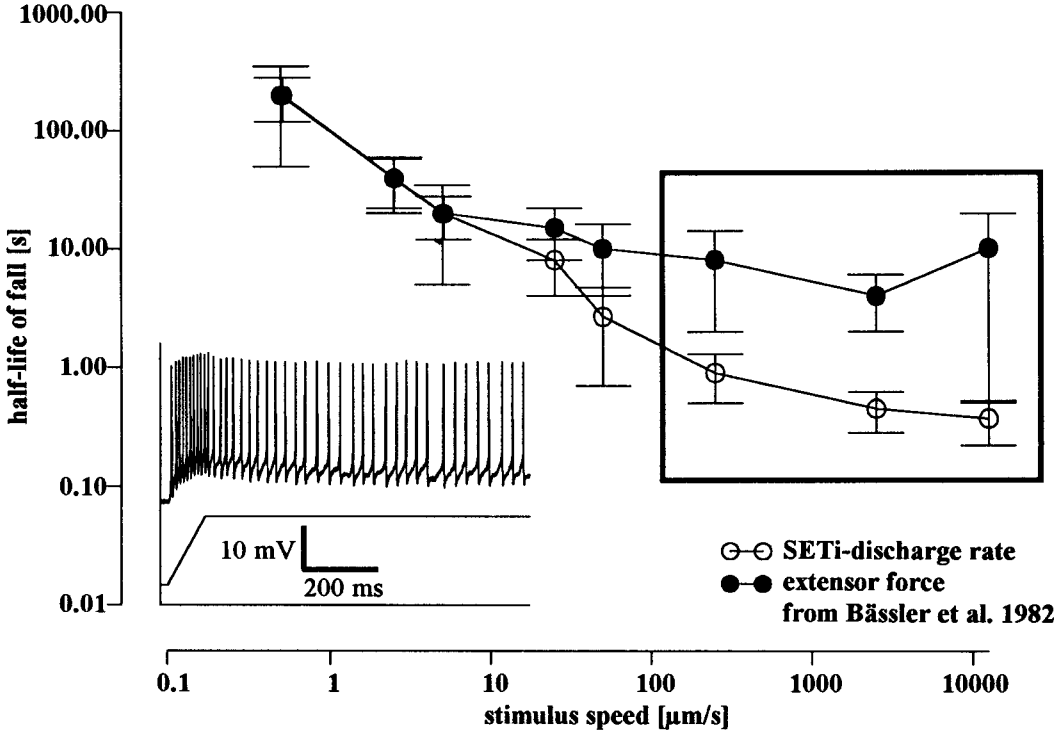

Fig. 1. Half-lives of decay in SETi-discharge rate and extensor force after the end of a ramp-wise elongation of the femoral chordotonal organ (amplitude: 400 µm), altered according to Bässler et al. (1982); *inset:* intracellular SETi-recording *(upper trace)* during such a stimulus *(lower trace)*. The *box* denotes the range of stimulus velocities tested in the present study

amplitude of depolarization of the excitatory extensor motor neurons and the shorter is the half-life of its decay (Fig. 1).

In the present paper we investigate whether these specific properties are generated (i) already at the level of single identified nonspiking interneurons presynaptic to the motor neurons (Büschges 1990) or (ii) solely at the level of the motor neurons as a consequence of the integration of their inputs. In the latter case it cannot be expected that the nonlinearity in the velocity dependence of the FT-control loop is already detectable at the interneuronal level.

We will show that the nonlinearity described above is already present in nonspiking interneurons in the FT-control loop.

Materials and methods

The experiments were carried out on adult, female stick insects of the species *Carausius morosus* from our colony at the university of Kaiserslautern. The animals were fixed dorsal side up on a platform. The middle legs, the meso- and metathoracic segments were placed in an enclosure (20 mm × 60 mm) filled with *Carausius* saline (Weidler and Diecke 1969). The femur of the left middle leg was fixed rectangular to the body, the tibia being rectangular to the femur. A small dorsal part (30%) of the cuticle of the femur was removed and the tendon of the extensor tibiae muscle was cut distally. The apodeme of the femoral chordotonal organ was fixed in a clamp and cut distally to the clamp. Flexion movements of the tibia were simulated by pulling the apodeme of the femoral chordotonal organ (starting position corresponding to 100° joint position) with an amplitude of either 100 µm or 400 µm (corresponding to joint movements from 100° to 80° and 100° to 20°, respectively; Weiland and Koch 1987). The stimuli were applied by a ramp-and-hold generator (for details of stimulation procedure see Büschges 1989). The applied stimulus velocities were in a range of 0.067 mm/s to 9.4 mm/s (13.4°/s to 1481.5°/s; Weiland and Koch 1987). The activity of the F2 nerve (innervating the extensor tibiae muscle) was recorded extracellularly by using a hook electrode (Schmitz et al. 1991). The nerve F2 contains the axons of FETi, SETi and of the common inhibitor 1 (CI_1) and the axons of a large number of sensory cells innervating tactile hairs. The recordings of this nerve were also a measure for the behavioral state of the animals. Only reactions that showed a clear resistance reflex of the extensor motoneurons in these recordings (Bässler 1983a; Fig. 1, inset) were used for further analysis.

Nonspiking interneurons that are part of the FT-control loop, types E1, E3, E4, E6 (Büschges 1990) were recorded in the dorsal, lateral neuropilar region of the mesothoracic ganglion. To receive stable recordings the mesothoracic ganglion was placed on a wax coated platform and fixed with cactus spines. It was then treated with Pronase E (Merck) for 40–80 s. Single electrode voltage clamp and current clamp recordings were performed to investigate whether intrinsic properties of nonspiking interneurons could be involved in the generation of the decay in the depolarizations. Therefore, most of the recordings were performed using a npi SEC1 L/H amplifier (npi electronic).

The electrodes used in non-voltage clamp recordings were thin walled (wpi) and filled with 4% Lucifer Yellow (tip solution) and 1 *M* LiCl (shaft solution; electrode resistance: 60–90 MΩ). The neurons were stained after physiological characterization by applying −1 to −3 nA constant current. After histological treatment the whole mounts were drawn using a camera lucida. For voltage and current clamp recordings the electrodes, also thin walled, were filled with 2 *M* KAc/0.05 *M* KCl (electrode resistance: 8–30 MΩ). With these electrodes a switching rate of 10 kHz and a VC gain of 1.5–2.5 (25% duty cycle) were routinely obtained. The true electrode potential was monitored separately. The interval between voltage samplings was always 15–25 times greater than the electrode time constant. Under these conditions ±7 nA of current could be applied with no visible rectification. The output bandwidth of the amplifier was generally set to 33 kHz.

Intracellular and extracellular signals, current and stimulus traces were recorded on an 8 channel DAT Recorder (biologic DTR-1800; sample rate 12 kHz) and analyzed off-line on a 33 MHz DOS 386 computer. The AD conversion was performed by using

a DT 2821/F 16SE AD/DA card and the program Turbolab V4.0 (Stemmer). The single channel sampling rate was set to 0.5 to 2 kHz for analyzing the intracellular recordings of the nonspiking interneurons and to 7.5 kHz for analyzing the extracellularly measured spike activity. The output files were converted with the program T1-spike (H. Hemker, O. Noack, T. Zäckel; V2.0) to perform further analysis with the program Spike2 (Cambridge electronics CO, Science Products, V3.14). This program was used for averaging the nonspiking interneuron responses and to produce peri stimulus time histograms (bin width: 10 ms) of the extracellular F2 recordings. In addition ASCII-files from averages and peri stimulus time histograms were produced and analyzed with the program Clampfit (FETCHEX™, Axon Instruments Inc, V5.5.1). Then, using Clampfit, exponential functions that described the time course of decay of motor neurons and interneurons were calculated. Each exponential function is characterized by its time constant τ and its coefficient A (see Equ. 1). The calculation of the coefficients A1 and A2 (of a double exponential function) for the SETi-activity was performed in another way: The value at the start of decay was taken as A1+A2 plus the tonic activity. A2 plus the tonic activity was calculated in each case as the average of the values of the fourth to the sixth class of the peri stimulus time histogram, 40 ms to 70 ms after start of the decay. The tonic activity (offset) was calculated as the average value of 10 classes of the peri stimulus time histogram 900 ms after the end of a given elongation stimulus and subtracted from the upper two values to obtain A1+A2 and A2 for the dynamic portion of the resistance reflex. A1 was then given by: (A1+A2)−A2 (further explanations in the Result part). The means and the standard deviations of the revealed time constants and coefficients for different animals were calculated. Significance was tested with the modified *t*-test – for $n<30$ and unequal variances – after Dixon and Massey (1969). Samples were considered to be significantly different at $P<0.05$.

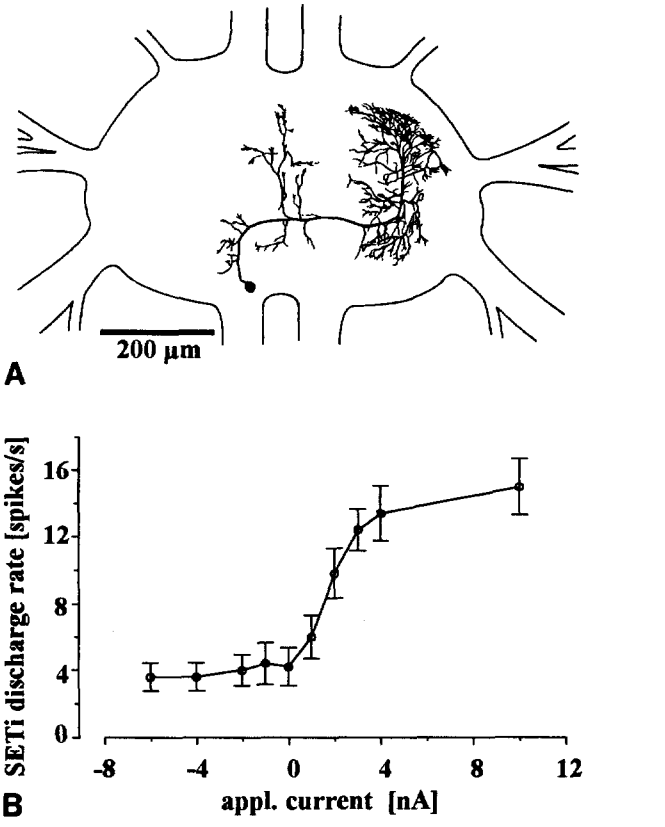

Fig. 2. Morphology (**A**) and output characteristics (**B**) of interneuron E4 (see text). S.D. is indicated. Each value is the average spike discharge rate of 10 s. *SETi* slow extensor tibiae motor neuron

Results

We particularly analyzed one type of nonspiking interneuron, E4, by quantitatively characterizing its response in the velocity range from 0.3–9.4 mm/s (see box in Fig. 1). It was chosen due to the strong velocity dependence of its response to femoral chordotonal organ stimulation (Büschges 1990). Additionally, E4 can be recognized unequivocally by its physiology. This is important for its identification in voltage clamp experiments with KAc-electrodes: In all cases depolarizing currents applied to E4 increased the discharge rate of the extensor motor neurons. Elongation as well as relaxation stimuli at the femoral chordotonal organ led to a depolarization in E4. The velocity threshold of responses to relaxation stimuli was greater than the one to elongation stimuli. The amplitude of the depolarizations to relaxation stimuli never exceeded the one to elongation stimuli. In more than 40 recordings (this paper; Büschges 1990; Driesang 1990) all neurons with such a physiology always had the same morphology.

Decay of membrane potential in E4 after elongation stimuli

Figure 2A shows the morphology of interneuron E4 according to Büschges (1990). The average resting membrane potential of interneurons E4 was -52.4 ± 3.9 mV ($n=10$ interneurons). Depolarizing currents applied to E4 through an intracellular electrode increased the discharge rate of the extensor motor neurons (in Fig. 2B shown for the SETi; Büschges 1990). As described above, E4 also receives afferent input during elongation of the femoral chordotonal organ (Fig. 3A). We were interested in the question whether in the FT-control loop the dependence of half-lives of decline on stimulus velocity is already apparent at the interneuronal level. Therefore, we quantitatively characterized the responses of interneurons E4 to elongation stimuli of the femoral chordotonal organ. Figure 3A shows that the amplitude of depolarizations increased with increasing stimulus velocity (Büschges 1990). Figure 3B demonstrates the changes in the average decline of the responses in E4 to elongation stimuli for 4 different stimulus velocities. A curve fitting program delivered exponential functions as being the best fit for the decline of the membrane potential (regression coefficient e.g. R: 0.88 for V=0.3 mm/s; R=0.99 for V=9.4 mm/s). For slow stimulus velocities (V=0.3 mm/s) a single exponential function was sufficient to describe the decay of depolarization in E4 ($\tau=190$ ms, Fig. 3B). For higher stimulus velocities a double exponential function was necessary to characterize the shape of the decay in the responses of E4 (Fig. 3, e.g. $\tau_1=16$ ms, $\tau_2=198$ ms, V=9.4 mm/s). This function is the sum of two exponential functions according to the following equation:

$$f(t) = A1*e^{\frac{-t}{\tau_1}} + A2*e^{\frac{-t}{\tau_2}} \quad (1)$$

τ_1 = the time constant of the fast decaying exponential function

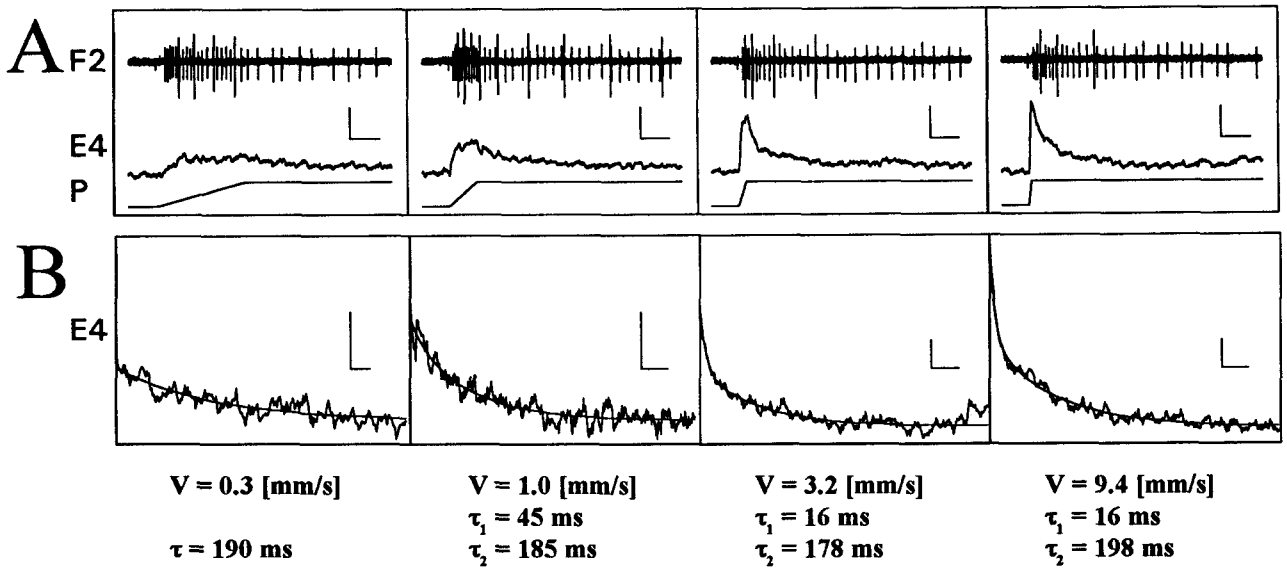

Fig. 3A, B. Responses of interneuron E4 to stimulation of the femoral chordotonal organ. E4 is depolarized by elongation of the femoral chordotonal organ and the amplitude of depolarization increased with increasing velocity (*V*; Büschges 1990). **A** Original recording from E4 and extensor nerve F2: *F2* Extracellular record from the extensor nerve (midsized spikes belong to SETi); *E4* intracellular record of interneuron E4; *P* stimulus. In this and all following figures an upward deflection of the stimulus trace corresponds to an elongation of the femoral chordotonal organ. The time scale is not extended enough to separate individual SETi spikes for higher stimulus velocities. SETi spike frequency increased with increasing stimulus velocity. **B** Averages of the decay of depolarization of 10 successive responses of an E4 neuron to the stimuli shown above. The best fit by exponential functions is indicated by *solid lines*. Time constants of best fits are given. Horizontal bar: 100 ms; vertical bar in **A**: 6 mV; **B**: 2 mV

τ_2 = the time constant of the slow decaying exponential function
A1 = contribution of the fast decaying exponential function to the amplitude
A2 = contribution of the slow decaying exponential function to the amplitude
Thus A1 + A2 for t = 0 gives the total amount of depolarization in the interneuron.

The same kind of analysis was performed for the recordings of altogether 17 interneurons E4. Each recording delivered, depending on stimulus velocity, one or two time constants (τ_1 and τ_2) and the corresponding coefficients (A1 and A2). All time constants (either τ_1 or τ_2) corresponding to a certain velocity were averaged. The result is summarized in Fig. 4A: For the slowest stimulus velocity (V = 0.3 mm/s) a single exponential function was always sufficient to describe the decay ($\tau_2 = 224.5 \pm 158$ ms). For higher stimulus velocities a double exponential function was always necessary. Statistical analysis revealed that the short time constants (τ_1) found for the different stimulus velocities were not significantly different. This was also true for the long time constants (τ_2). This means that the values of both time constants were independent of stimulus velocity. Whenever two time constants were found at one stimulus velocity, τ_1 and τ_2 were significantly different.

The shape of the decline of a double exponential function also depends on the coefficients (A1, A2) of each exponential function (see above). A1 gives the relative contribution of the exponential function with the short time constant τ_1. A2 gives the relative contribution of the exponential function with the long time constant τ_2. Those contributions (A1, A2) were analyzed as follows: At first the value of A1 + A2 at a velocity of 9.4 mm/s (the maximum response amplitude) was set 1 for each of the recorded neurons and all amplitude values were normalized to this value. A1 was zero at a stimulus velocity of 0.3 mm/s and increased with increasing stimulus velocity (Fig. 4B). In contrast the coefficient A2 was similar for all tested stimulus velocities and did not change with stimulus velocity (Fig. 4B). That means that the relative contribution of A1 increased with increasing velocity. Therefore, the characteristic of the fast decaying exponential function (τ_1) dominated more and more with increasing stimulus velocity (Fig. 4A inset, Fig. 4B).

So far our results have shown that the decay of the depolarization in E4 following an elongation stimulus at the femoral chordotonal organ was best fit by one exponential function for slow stimulus velocities and by two exponential functions for higher stimulus velocities. The contribution of each function to the amount of depolarization depended on stimulus velocity.

How can this feature explain the properties of the motor output as described by Bässler et al. (1982, Fig. 1)? In their study only the half-lives of decay were evaluated (Fig. 1). If we had analyzed the half-lives of decay for the depolarizations in E4 we also would have found a decrease in the half-life of decay with increasing stimulus velocity. This is obvious from the inset shown in Fig. 4A. That means that a nonlinearity concerning the dependence of half-lives on stimulus velocity existed at the level of interneurons of type E4. The remaining questions were: Are the properties shown for interneuron E4 in the same parameter range as those of the motor output? Are similar properties present in other types of interneurons? What kind of mechanisms underly this phenomenon?

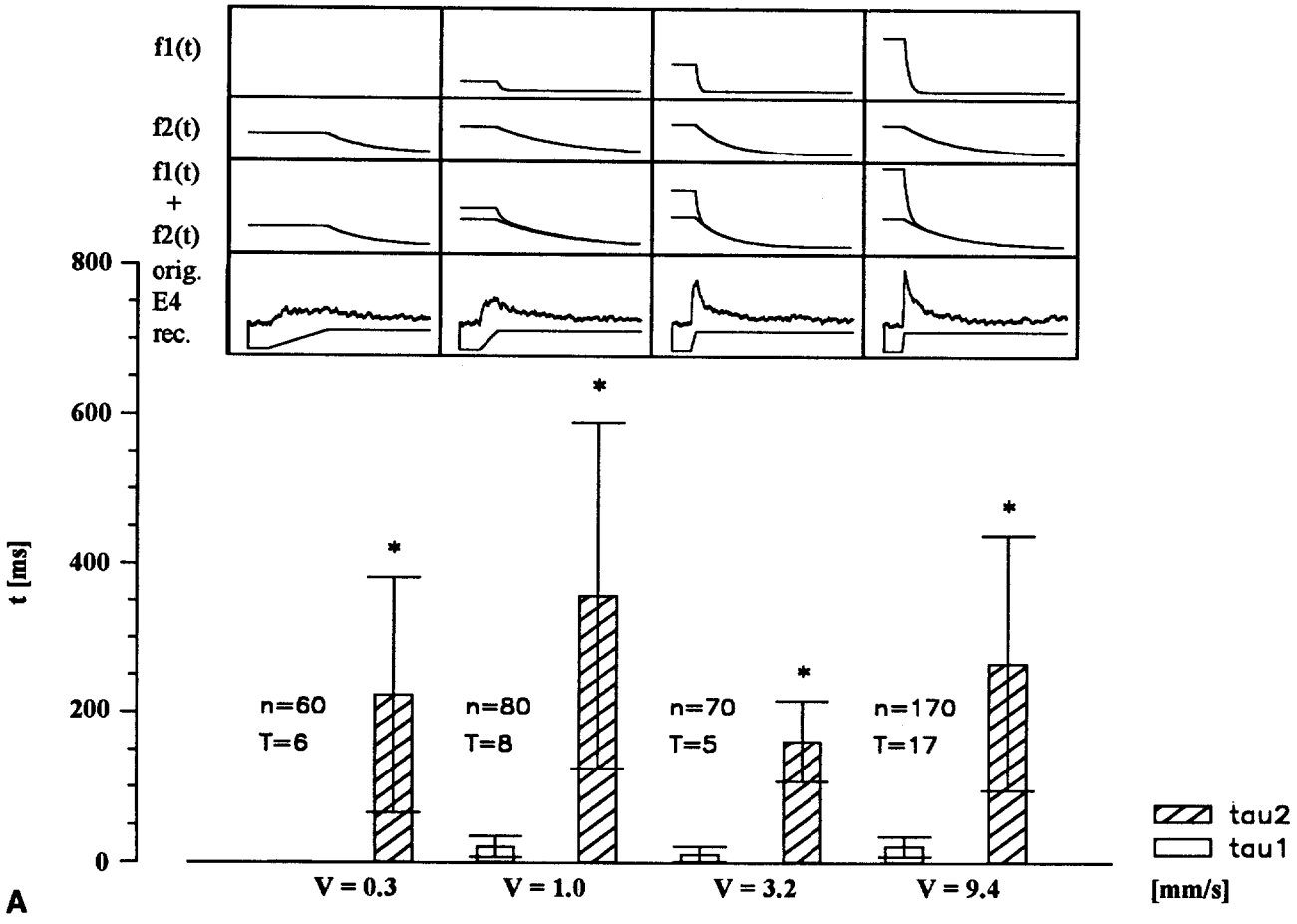

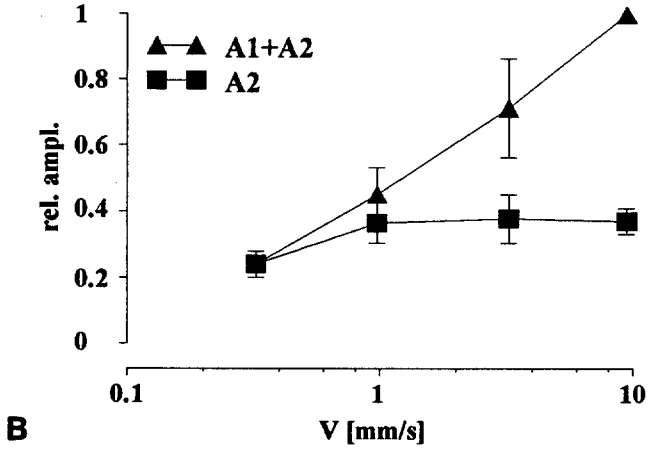

Fig. 4. A Quantitative comparison of the time constants of the best fit functions for the decline of the responses in E4 after a ramp-wise elongation of the femoral chordotonal organ: Means and standard deviations of the time constants of the exponential functions for 4 different stimulus velocities (V) are given. *n* number of evaluated stimuli; *T* number of evaluated E4-neurons. *Asterisks* mark significant differences between τ_1 and τ_2. The *inset* shows effects of both exponential functions on decline of depolarizations in E4. In the top row a single exponential function demonstrating the contribution of the fast decaying function is given: $f1(t) = A1 * e^{\frac{-t}{\tau_1}}$ the second row denotes the contribution of the slow decaying function $f2(t) = A2 * e^{\frac{-t}{\tau_2}}$. The third row shows the sum of f1(t) + f2(t) and for comparison the bottom row shows the averages of an original record of E4 (for details see text). **B** Dependence of A1 and A2 on stimulus velocity in interneuron E4. Mean and standard errors of the normalized amplitude values (A1 and A2) are given (for details see text). A2 *(filled squares)* is constant for all tested stimulus velocities. Accordingly, A1 + A2 *(filled triangles)* increased with increasing velocity

Comparison with the motor output

Since Bässler et al. (1982) did not use computer calculations to reveal best fit functions of the motor output (muscle force and SETi activity) it is difficult to compare their results with the values found here. Therefore, we reinvestigated the time course of SETi activity in response to chordotonal organ stimulation in the same velocity range as we did for E4. The calculations of the time constants of the decay in the SETi response to elongation stimuli were performed in the following way: First, a peri stimulus time histogram (bin width 10 ms) was calculated for several successive stimuli ($n = 10$ for the case that the SETi was recorded parallel to E4; *n* from 50 to 90 when the SETi-activity alone was measured, see below). The plot of this histogram was tested

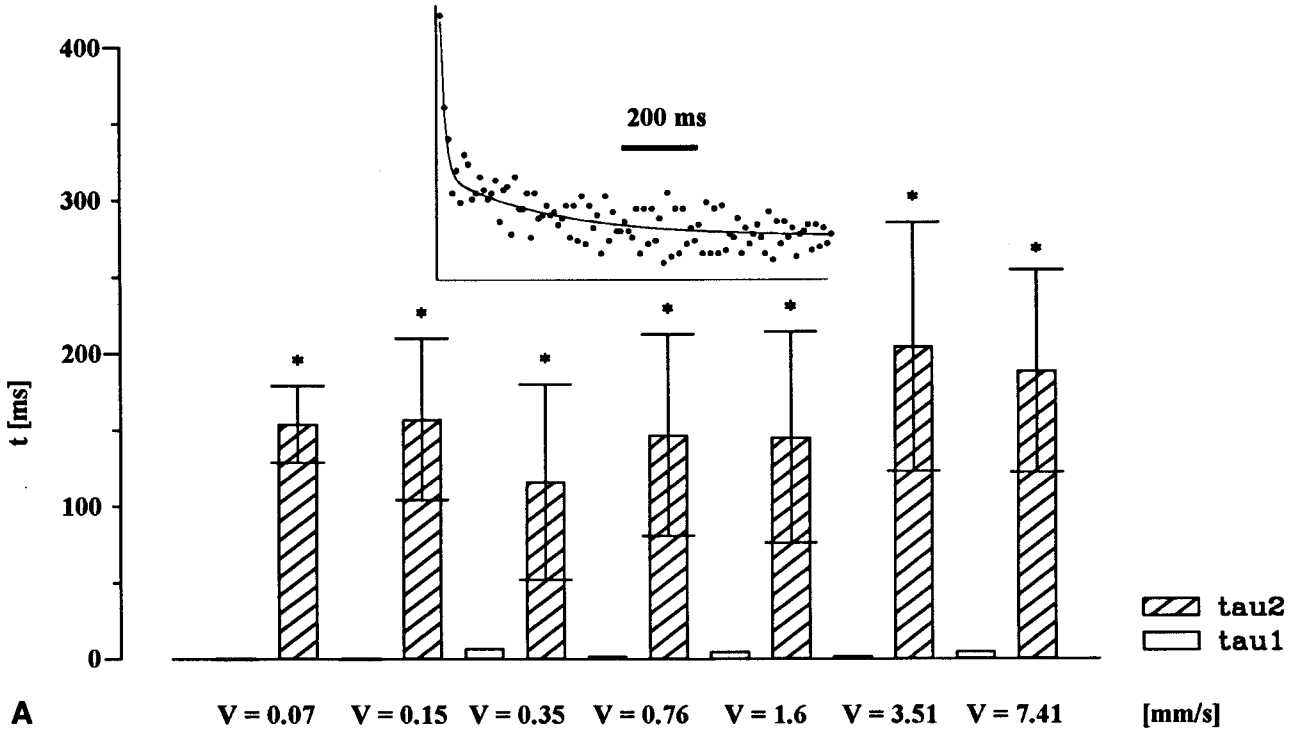

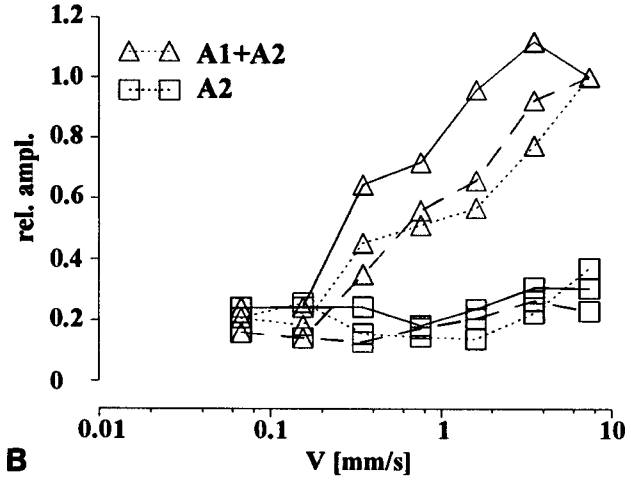

Fig. 5. A Average time constants of the decline in SETi discharge rate after a ramp-wise elongation of the femoral chordotonal organ for different stimulus velocities (*V*). Means and standard deviations. The standard deviations for τ_1 were too small for being depicted. An *asterisk* indicates that τ_1 and τ_2 are significantly different for a distinct velocity value. *Inset:* Peri stimulus time histogram of SETi responses to 50 successive stimulations of the femoral chordotonal organ at a velocity of 7.4 mm/s. For details see text. **B** Dependence of the normalized amplitude values (A1, A2) of the decay in SETi-discharge on stimulus velocity for three animals (see Fig. 4B). Note that A2 *(open squares)* is almost constant over the tested range of velocity. A1 and therefore the sum of A1 + A2 *(open triangles)* increased with increasing stimulus velocity

for a fit by either single or double exponential functions, respectively (Fig. 5A inset). This procedure delivered the time constants (τ_1 and τ_2) and the coefficients (A1 and A2, see Materials and methods).

(i) The characteristics of the SETi activity were investigated in detail in 3 animals (Fig. 5): The decay of activity in SETi following a stimulus with slow velocity (V = 0.067 mm/s) could be described by a single exponential function (τ: range 152–180 ms), the decay of activity following higher stimulus velocities by a double exponential function. Whenever two time constants were found for a certain stimulus velocity, they were significantly different (Fig. 5A). The values of the time constants of SETi were in a similar range as has been shown for interneuron E4 (see below). The coefficients A1 and A2 of the exponential functions were again normalized to the value of A1 + A2 at a velocity of 7.4 mm/s. A1 was zero for small velocities ($V \leq 0.15$ mm/s) and increased markedly with increasing stimulus velocity. A2 only showed a bare increase with stimulus velocity (Fig. 5B). That means that the relative contribution of A1 increased with increasing stimulus velocity. Therefore, the corresponding exponential function with the short time constant (τ_1) dominated with higher stimulus velocities, as has been shown for interneuron E4.

(ii) We investigated as well the time constants for E4 and SETi in the same animal in 5 experiments. The results showed that in a single animal the time constants were similar for E4 and SETi (e.g. $\tau_1 = 13 \pm 7$ ms (E4), $\tau_1 = 7 \pm 6$ ms (SETi); $\tau_2 = 189 \pm 45$ ms (E4), $\tau_2 = 207 \pm 66$ ms (SETi), V = 9.4 mm/s). That means that the time course of decay is equal for SETi activity and E4 membrane potential.

Characteristics of other nonspiking interneurons

In addition we investigated three other types of nonspiking interneurons in the FT-control loop: E1, E3 und E6 (Fig. 6; Büschges 1990). They all are depolarized by elongation stimuli at the femoral chordotonal organ and are excitatorily coupled to the extensor motor neurons. Thus, they contribute to SETi excitation during imposed flexion of the FT-joint. For higher stimulus velocities all these interneurons showed a decay of the depolarization after a stimulus at the femoral chordotonal organ that followed a double exponential function. The time constants (Fig. 6) were in the same order of magnitude as those of interneuron E4. It was not investigated whether the coefficients A1 and A2 depend in the same way on stimulus velocity as in E4.

Single electrode voltage clamp and current clamp analysis

Rectangular current pulses ($n = 10$–20, from 0 to -1 nA, duration: 1.5 s) were applied to interneuron E4 in the current clamp mode to investigate the passive membrane time constants (Fig. 7). The time course of the decay after the end of the stimulus was analyzed. We found two time constants: The first time constant was 3.4 ± 2.1 ms, the second one 50.4 ± 24.7 ms ($n = 5$ E4 neurons). The first time constant describes the equalizing current, the second the membrane time constant (Rall 1969). This passive membrane time constant τ_{pas} was significantly different from the value of the short time constant (τ_1) and from the value of the long time constant (τ_2) described for the decay in the repolarization after afferent input to interneuron E4. This indicated that either voltage dependent properties of the interneuronal membrane or properties of the inputs to the interneuron are responsible for the time constants τ_1 and τ_2.

If the described characteristics of the decay of depolarizations in E4 were a consequence of its intrinsic properties, the time course of decay would change if the membrane potential was artificially shifted away from resting potential (Laurent 1990). In contrast, if the time course of the decay would be caused by inputs, no change should be observed (Laurent and Sivaramakrishnan 1992). To test this the following experiments were performed: (1) We injected constant current in interneuron E4 under current clamp conditions in a range of -3 to $+2$ nA. Simultaneously the femoral chordotonal organ was stimulated. The analysis revealed that the time course of the membrane potential was independent of the applied current (Fig. 8).

(2) We compared the time course of membrane potential and membrane current in E4 following afferent input from the femoral chordotonal organ. Figure 9A shows the response of interneuron E4 to a ramp-and-hold stimulus during bridge mode recording conditions at resting potential (upper trace: voltage trace, average of 10 sweeps). The middle trace shows the (inverted) inward current under voltage clamp conditions for the same neuron E4 (average of 10 sweeps). The holding potential in the voltage clamp mode was set to -70 mV and thus

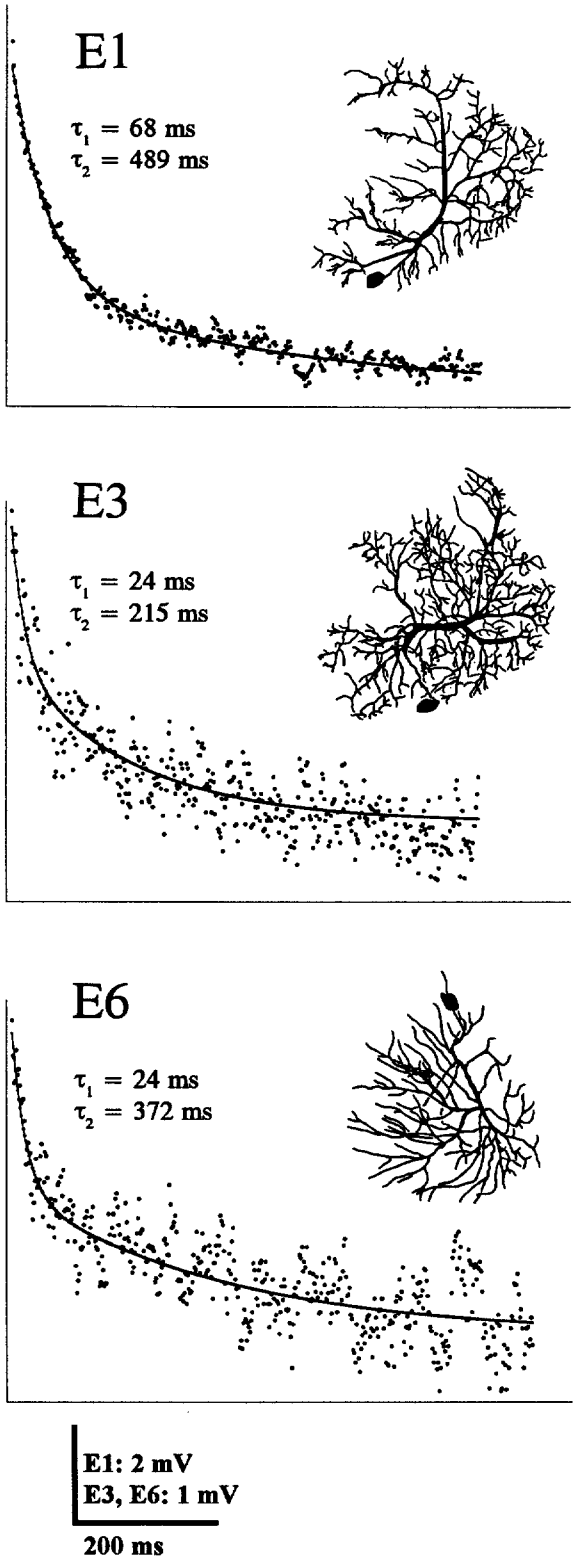

Fig. 6. Average decline of the depolarization after a ramp-wise elongation of the femoral chordotonal organ in three other types of nonspiking interneurons: E1, E3 and E6 (according to Büschges 1990, morphology is given in *inset*, all neurons are drawn with the same magnification). The *solid lines* show the best fit by double exponential functions whose time constants τ_1 and τ_2 are specified

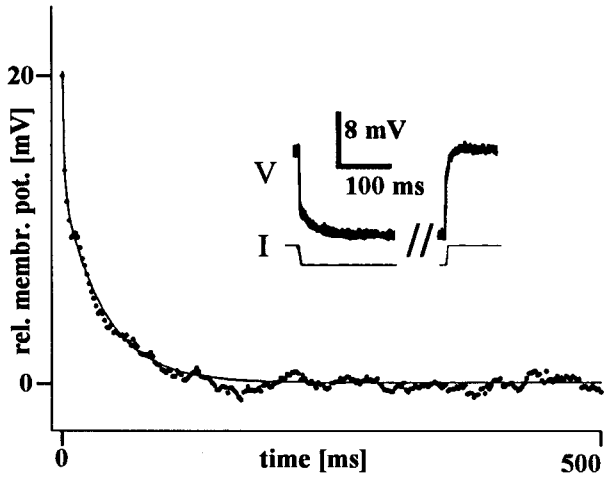

Fig. 7. Determination of the passive and equalizing time constants in E4. Current pulses of 0 nA to −1 nA were applied in the current clamp mode (10 to 20 sequences, holding time 1.5 s). The same program that was used to calculate the time course of decay in the E4 responses (see Materials and methods) was used to calculate the exponential functions of the decay in membrane potential after a current drop from 0 nA to −1 nA. The decay of membrane potential was best described by the following double exponential function: $f(t) = A1*e^{\frac{-t}{4.1}} + A2*e^{\frac{-t}{92.9}}$, $R = 0.98$, τ in ms. Inset: 12 superimposed sweeps of membrane potential (V) and current trace (I), current pulse from 0 nA to −1 nA

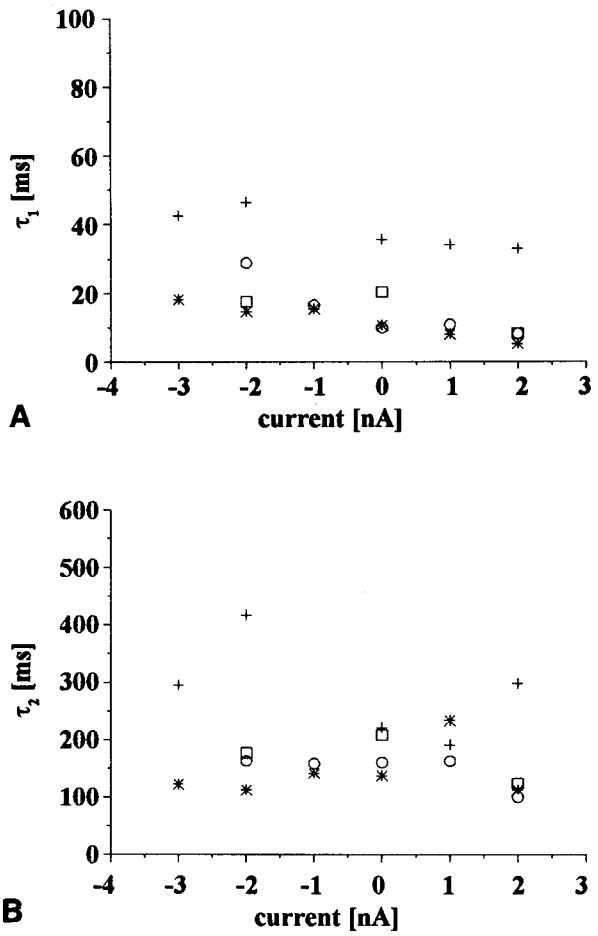

Fig. 8. Time constants τ_1 (**A**) and τ_2 (**B**) of responses in E4 in the current clamp mode. Constant current in the range of −3 nA to +2nA was applied in 4 recordings. Simultaneously the femoral chordotonal organ was stimulated (amplitude: 400 µm, velocity: 7.4 mm/s) and the decay of the responses of E4 was analyzed as described above. Note the *different symbols* for the different recordings, each *point* represents the average of 10 responses

about 20 mV below resting potential. Double exponential fits for both curves revealed almost equal time constants: $\tau_1 = 10$ ms and $\tau_2 = 126$ ms for the voltage trace and $\tau_1 = 9$ ms and $\tau_2 = 149$ ms for the current trace. This was tested for altogether four recordings (Fig. 9B).

That means that the membrane potential of interneuron E4 exactly followed the membrane current. Therefore voltage-dependent membrane properties like the transient "A" -current (Hagiwara et al. 1961; Connor and Stevens 1971; Byrne 1980) or the delayed-rectifier current cannot be involved in the generation of the time course of decay in E4. Thus the membrane current corresponds to the synaptic current representing the neuron's input (Laurent and Sivaramakrishnan 1992).

Discussion

The physiology of interneurons in the FT-control loop is sufficient to explain the motor output

We have shown that properties of the FT-control loop being essential for the generation of catalepsy are already apparent at the level of a single identified nonspiking interneuron: The amplitude of the depolarizations induced by elongation of the femoral chordotonal organ increased with increasing stimulus velocity. Depending on stimulus velocity the decay of these depolarizations could be described by single or double exponential functions. The time constants (τ_1, τ_2) were significantly different from each other and independent of stimulus velocity (Fig. 4A). We found comparable properties in other nonspiking interneurons as well (E1, E3, E6; Büschges 1990). The time constant of the single exponential function was in the range of the long time constant (τ_2) of the double exponential function. The amplitude of the slowly decaying function (A2) was independent of stimulus velocity. The essential change in the depolarization of interneuron E4 with increasing stimulus velocity was the increase of the coefficient A1 (Fig. 4A inset, Fig. 4B). That means that the decay of the membrane potential in interneurons E4 was faster for higher velocities than for lower ones.

For the slow extensor tibiae motor neuron (SETi) the same characteristics in the decay following ramp-wise elongation of the femoral chordotonal organ were found. That means that characteristics of single identified nonspiking interneurons in the FT-control loop are already sufficient to explain specific properties of the motor output. This means furthermore, that although the integration and summation of inputs in the motor neurons might contribute to the time course of the response, it is not necessary for it. In addition, our results indicate that potentially existing monosynaptic connections from afferents of the femoral chordotonal organ onto motor neurons, as described for the locust (Burrows 1987a),

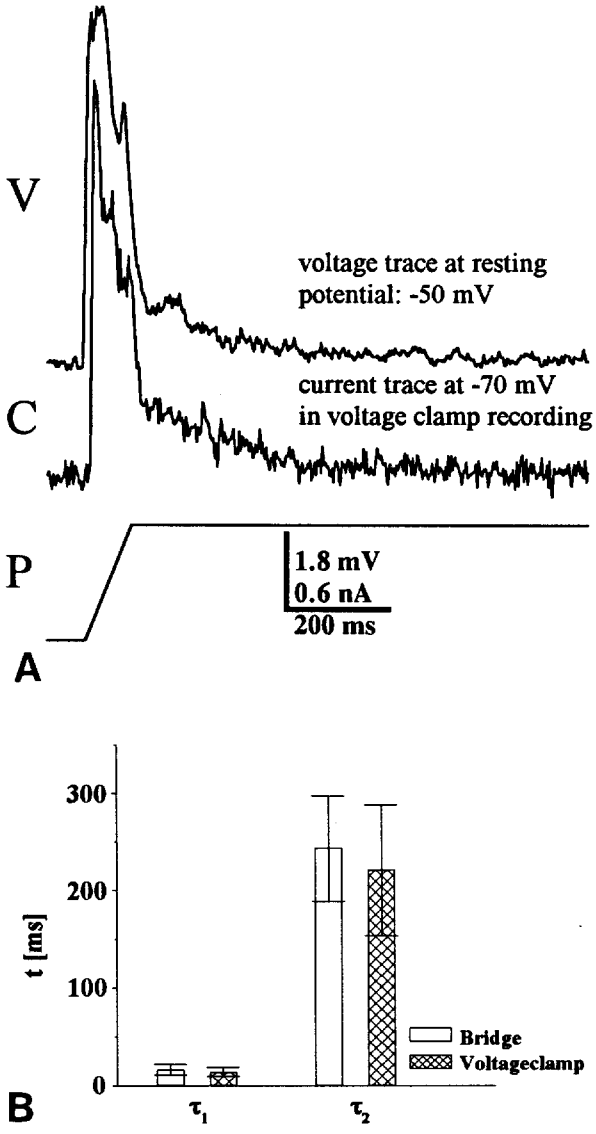

Fig. 9A, B. Analysis of the time constants of the current following afferent input to E4 in voltage clamp mode. Comparison with bridge mode recordings. **A** The femoral chordotonal organ was stimulated by ramp-wise elongation. The upper trace shows the average of 10 responses of an E4 neuron in the bridge mode at resting potential (ca. −50 mV, voltage trace, *V*). The decay of this trace was fit by a double exponential function. The revealed time constants were: $\tau_1 = 10$ ms, $\tau_2 = 126$ ms, R = 0.96. The middle trace shows the average of 10 responses of the same neuron to the same stimulus under voltage clamp conditions at a holding potential of −70 mV (current trace is inverted for better comparison, *C*). This trace was as well fit by a double exponential function. The revealed time constants were: $\tau_1 = 9$ ms, $\tau_2 = 149$ ms, R = 0.99. Bottom trace: stimulus, *P*. **B** The above evaluation procedure was repeated in four recordings. The means evaluated for the respective time constants showed no significant difference between the recordings in bridge- and voltage clamp mode

would not be necessary for the generation of the properties in the FT-control loop that enable the system to produce catalepsy.

However, our findings cannot be interpreted in a way that a resistance reflex produced by the FT-control loop to imposed joint movements is solely generated by so called "resisting" pathways. It is known that the neural networks controlling leg joints in the stick insect contain both "resisting" and "assisting" pathways affecting the motor output of the system (Büschges 1990; Büschges and Schmitz 1991; for detailed review see Bässler 1993). This situation does not interfere with our results, because the question that has been answered in the current study was as to whether specific properties of a joint control loop would be apparent already at the level of single premotoric nonspiking interneurons.

Mechanisms underlying the time course of decay in interneuron E4

Voltage clamp analysis revealed that after an elongation stimulus the time course of the current across the membrane is equivalent to the time course of the membrane potential as evaluated in bridge mode (Fig. 9). In addition current clamp recordings showed that the time constants were independent of the applied current (Fig. 8). That means that, at least at the recording site, no voltage-dependent channels were involved in the generation of the two time constants.

At the moment it therefore appears highly likely that the time course of the inputs to E4 neurons are the relevant factors for the generation of its specific properties. Those specific inputs are currently not known in detail. In the locust exist direct sensory inputs from femoral chordotonal organ afferents onto local interneurons and indirect inputs onto them via intercalated interneurons (Burrows 1987b, 1989). Therefore it is conceivable that interneuron E4 in the stick insect might also be reached via two different pathways. Their influence might be expressed as A1 and A2 in the response of E4.

The observed short time constant (τ_1) in the response of E4 was shorter than the passive membrane time constant (τ_{pas}). Therefore, we have to postulate a complex character of these inputs: The depolarization can simply be produced by depolarizing synaptic currents, but the decay cannot simply be the result of switching off these currents. Instead, special repolarizing factors must exist. These factors would be present if the inputs to interneuron E4 involved multiaction-synapses (Getting 1981; Kehoe 1972) or if excitatory and inhibitory synapses acted in parallel on E4. In the latter case the inhibition, occurring with a greater latency and higher threshold, could then lead to the fast repolarization (τ_1). This would explain τ_1 being smaller than τ_{pas}.

Comparison with other systems

The neural basis of joint control loops has been investigated quite successfully in a number of model systems, particularly in invertebrates, like the crayfish (e.g. El Manira et al. 1991a, b), the locust (for review see: Burrows 1989) or the stick insect (for review see: Bässler 1993; Büschges 1990). In most cases the generation of resistance reflexes has been studied with the goal of elucidating the "wiring diagram" of the neural networks underlying joint control loops (Burrows et al. 1988; Burrows 1989, 1992). However, for most systems it still remains unknown what specific information is processed

in a particular pathway of the circuit and how the described pathways contribute to the characteristics of the whole system. Our goal was different: We tried to analyze the physiology of an identified neuron beyond its contribution given by its incorporation in the neural circuitry transmitting sensory information onto the motor neurons. We could show that specific properties of the FT-control loop enabling the leg joint to produce the behavior of catalepsy are already apparent at the interneuronal level.

This finding contradicts to some extent the results on the generation of resistance reflexes in the crayfish. El Manira et al. (1991a) have shown that sensory neurons of the coxo-basipodite chordotonal organ make monosynaptic connections to levator and depressor motor neurons of the joint that would be appropriate for the generation of resistance reflexes to imposed movements. Based on their study of connectivity it is currently inferred that resistance reflexes in the crayfish are mainly mediated via monosynaptic connections from sense organs to the motor neurons of a joint (El Manira et al. 1991a). According to our results this situation would differ significantly from the one in the stick insect.

Acknowledgements. We thank Prof U. Bässler for his steady support. We thank U. Bässler and A. Sauer for valuable discussions and their criticism on an earlier draft of this manuscript. This work was supported by DFG (Ba 578).

References

Bässler U (1983a) Neural basis of elementary behavior in stick insects. Springer, Berlin Heidelberg New York

Bässler U (1983 b) The neural basis of catalepsy in the stick insect *Cuniculina impigra* 3. Characteristic of the extensor motor neurons. Biol Cybern 46:159–165

Bässler U (1992) Variability of femoral chordotonal organ reflexes in the locust, *Locusta migratoria*. Physiol Entomol 17:208–212

Bässler U (1993) The femur-tibia control system of stick insects – a model system for the study of the neural basis of joint control. Brain Res Rev 18:207–226

Bässler U, Foth E (1982) The neural basis of catalepsy in the stick insect *Cuniculina impigra* 1. Catalepsy as a characteristic of the femur-tibia control system. Biol Cybern 45:101–105

Bässler U, Storrer J, Saxer K (1982) The neural basis of catalepsy in the stick insect *Cuniculina impigra* 2. The role of the extensor motor neurons and the characteristics of the extensor tibiae muscle. Biol Cybern 46:1–6

Büschges A (1989) Processing of sensory input from the femoral chordotonal organ by spiking interneurones of stick insects. J Exp Biol 144:81–111

Büschges A (1990) Nonspiking pathways in a joint-control loop of the stick insect *Carausius morosus*. J Exp Biol 151:133–160

Büschges A, Schmitz J (1991) Nonspiking pathways antagonize the resistance reflex in the thoraco-coxal joint of stick insects. J Neurobiol 22(3):224–237

Burrows M (1987a) Parallel processing of proprioceptive signals by spiking local interneurons and motor neurons in the locust. J Neurosci 7(4):1064–1080

Burrows M (1987b) Inhibitory interactions between spiking and nonspiking local interneurons in the locust. J Neurosci 7(10):3282–3292

Burrows M (1989) Proccessing of mechanosensory signals in local reflex pathways of the locust. J Exp Biol 146:209–227

Burrows M (1992) Local circuits for the control of leg movements in an insect. Trends Neurosci 15(6):226–232

Burrows M, Laurent G, Field LH (1988) Proprioceptive inputs to nonspiking local interneurons contribute to local reflexes of a locust hindleg. J Neurosci 8:3085–3093

Byrne JH (1980) Analysis of ionic conductance mechanisms in motor cells mediating inking behavior in *Aplysia californica*. J Neurophysiol 43(3):630–650

Connor JA, Stevens CF (1971) Voltage-clamp study of a transient outward membrane current in the gastropod neural somata. J Physiol (Lond) 213:21–30

Dixon WJ, Massey FJ (1969) Introduction to statistical analysis. 3rd edition, McGraw Hill, New York

Driesang RB (1990) Nichtspikende Interneurone im Femur-Tibia-Regelkreis der Stabheuschrecke *Carausius morosus*. Master's thesis, Univ. Kaiserslautern, Germany

El Manira A, Caettert D, Clarac F (1991a) Monosynaptic connections mediate resistance reflex in crayfish *(Procambarus clarkii)* walking legs. J Comp Physiol A 168:337–349

El Manira A, DiCaprio RA, Cattaert D, Clarac F (1991b) Monosynaptic interjoint reflexes and their central modulation during fictive locomotion in crayfish. Eur J Neurosci 3:1219–1231

Getting PA (1981) Mechanisms of pattern generation underlying swimming in *Tritonia*. I. Neuronal network formed by monosynaptic connections. J Neurophysiol 46(1):65–79

Godden DH (1974) The physiological mechanisms of catalepsy in the stick insect *Carausius morosus* Br. J Comp Physiol 89:251–274

Harris-Warrick RM, Marder E, Selverston AI, Moulins M (eds) (1992) Dynamic biological networks. MIT Press, Massachusetts Institute of Technology; Cambridge, Massachusetts

Hagiwara S, Kusano K, Saito N (1961) Membrane changes of *Onchidium* nerve cell in potassium-rich media. J Physiol (Lond) 155:470–489

Kehoe J (1972) The physiological role of three acetycholine receptors in synaptic transmission in *Aplysia*. J Physiol (Lond) 225:147–172

Laurent G (1990) Voltage-dependent nonlinearities in the membrane of locust nonspiking local interneurons, and their significance for synaptic integration. J Neurosci 10(7):2268–2280

Laurent G, Sivaramakrishnan A (1992) Single local interneurons in the locust make central synapses with different properties of transmitter release on distinct postsynaptic neurons. J Neurosci 12(6):2370–2380

Rall W (1969) Time constants and electrotonic length of membrane cylinders and neurons. Biophys J 9:1483–1508

Ritzmann RE, Pollack AJ (1990) Parallel motor pathways from thoracic interneurons of the ventral giant interneuron system of the cockroach, *Periplaneta americana*. J Neurobiol 21(8):1219–1235

Robertson RM, Pearson KG (1985) Neural circuits in the flight system of the locust. J Neurophysiol 53(1):110–128

Schmitz J, Delcomyn F, Büschges A (1991) Oil and hook electrodes for en passant recording from small nerves. In: Conn PM (ed) Methods in neuroscience 4. Academic Press, San Diego New York Boston, pp 266–278

Weidler DJ, Diecke FPJ (1969) The role of cation conduction in the central nervous system in the herbivorous insect *Carausius morosus*. Z Vergl Physiol 64:372–399

Weiland G, Koch UT (1987) Sensory feedback during active movements of stick insects. J Exp Biol 133:137–156

Wolf H (1991) Sensory feedback in locust flight patterning. In: Armstrong DM, Bush BMH (eds) Locomotor neural mechanisms in arthropods and vertebrates. Manchester Univ. Press, pp 134–148